Investigating the influences of the precise manufactured shape of dipole nanoantennas on their optical properties

C. Moosmann, G. S. Sigurdsson, M. D. Wissert, K. Dopf, U. Lemmer, and H.-J. Eisler*

Nanoscale Science Group, Light Technology Institute (LTI), Karlsruhe Institute of Technology, 76131 Karlsruhe, Germany

hans.eisler@kit.edu

Abstract: Fabrication of small nanoantennas with high aspect ratios via electron beam lithography is at the current technical limit of nanofabrication and hence significant deviations from the intended shape of small nanobars occur. Via numerical simulations, we investigate the influence of geometrical variations of gap nanoantennas, having dimensions on the order of only a few tens of nanometers. We show that those deviations have a significant influence on the performance of such nanoantennas. In particular, their resonance wavelength as well as the magnitude of absorption and scattering cross section and the electric field distribution in the near field is strongly altered. Our findings are thus of importance for applications based on near field as well as those based on far field interactions with nanoantennas and have to be carefully and individually considered in both cases.

References and links

1. E. Ozbay, "Plasmonics: Merging photonics and electronics at nanoscale dimensions," Science **311**, 189–193 (2006).
2. S. A. Maier and H. A. Atwater, "Plasmonics: Localization and guiding of electromagnetic energy in metal/dielectric structures," J. Appl. Phys. **98**, 011101 (2005).
3. J. A. Schuller, E. S. Barnard, W. Cai, Y. C. Jun, J. S. White, and M. L. Brongersma, "Plasmonics for extreme light concentration and manipulation," Nat. Mater. **9**, 193–204 (2010).
4. K. Busch, G. von Freymann, S. Linden, S. F. Mingaleev, L. Tkeshelashvili, and M. Wegener, "Periodic nanostructures for photonics," Phys. Rep. **444**, 101–202 (2007).
5. J. N. Anker, W. P. Hall, O. Lyandres, N. C. Shah, J. Zhao, and R. P. Van Duyne, "Biosensing with plasmonic nanosensors," Nat. Mater. **7**, 442–453 (2008).
6. E. A. Coronado and G. C. Schatz, "Surface plasmon broadening for arbitrary shape nanoparticles: A geometrical probability approach," J. Chem. Phys. **119**, 3926–3934 (2003).
7. P. Mühlschlegel, H.-J. Eisler, O. J. F. Martin, B. Hecht, and D. W. Pohl, "Resonant optical antennas," Science **308**, 1607–1609 (2005).
8. J. N. Farahani, D. W. Pohl, H.-J. Eisler, and B. Hecht, "Single quantum dot coupled to a scanning optical antenna: A tunable superemitter," Phys. Rev. Lett. **95**, 017402 (2005).
9. A. Kinkhabwala, Z. F. Yu, S. H. Fan, Y. Avlasevich, K. Müllen, and W. E. Moerner, "Large single-molecule fluorescence enhancements produced by a bowtie nanoantenna," Nat. Photonics **3**, 654–657 (2009).
10. T. Klar, M. Perner, S. Grosse, G. von Plessen, W. Spirkl, and J. Feldmann, "Surface-plasmon resonances in single metallic nanoparticles," Phys. Rev. Lett. **80**, 4249–4252 (1998).
11. T. Taminiau, F. Stefani, F. Segerink, and N. F. van Hulst, "Optical antennas direct single-molecule emission," Nat. Photonics **2**, 234–237 (2008).

12. J. J. Greffet, M. Laroche, and F. Marquier, "Impedance of a nanoantenna and a single quantum emitter," Phys. Rev. Lett. **105**, 117701 (2010).
13. L. Novotny, "Effective wavelength scaling for optical antennas," Phys. Rev. Lett. **98**, 266802 (2007).
14. E. Seo, B. K. Choi, and O. Kim, "Determination of proximity effect parameters and the shape bias parameter in electron beam lithography," Microelectron. Eng. **53**, 305–308 (2000).
15. M. Hauptmann, K. H. Choi, P. Jaschinsky, C. Hohle, J. Kretz, and L. M. Eng, "Determination of proximity effect parameters by means of CD-linearity in sub 100nm electron beam lithography," Microelectron. Eng. **86**, 539–543 (2009).
16. A. V. Kildishev, J. D. Borneman, K.-P. Chen, and V. P. Drachev, "Numerical modeling of plasmonic nanoantennas with realistic 3D roughness and distortion," Sensors **11**, 7178–7187 (2011).
17. A. M. Kern and O. J. F. Martin, "Excitation and reemission of molecules near realistic plasmonic nanostructures," Nano Lett. **11**, 482–487 (2011).
18. A. Trügler, J.-C. Tinguely, J. R. Krenn, A. Hohenau, and U. Hohenester, "Influence of surface roughness on the optical properties of plasmonic nanoparticles," Phys. Rev. B **83**, 081412 (2011).
19. "http://www.lumerical.com," (2012).
20. "http://www.comsol.com," (2012).
21. H. Fischer and O. J. F. Martin, "Engineering the optical response of plasmonic nanoantennas," Opt. Express **16**, 9144–9154 (2008).
22. Raith GmbH, personal communication (2011).
23. M. D. Wissert, A. W. Schell, K. S. Ilin, M. Siegel, and H.-J. Eisler, "Nanoengineering and characterization of gold dipole nanoantennas with enhanced integrated scattering properties," Nanotechnology **20**, 425203 (2009).
24. O. C. Zienkiewicz, R. L. Taylor, and J. Z. Zhu, *Finite Element Method: Its Basis and Fundamentals* (Butterworth Heinemann, 2005).
25. A. Taflove and S. C. Hagness, *Computational Electrodynamics: The Finite-Difference Time-Domain Method* (Artech House Inc, 2005).
26. P. B. Johnson and R. W. Christy, "Optical-constants of noble-metals," Phys. Rev. B **6**, 4370–4379 (1972).
27. M. Fleischmann, P. J. Hendra, and A. J. McQuillian, "Raman-spectra of pyridine adsorbed at a silver electrode," Chem. Phys. Lett. **26**, 163–166 (1974).
28. K. T. Shimizu, W. K. Woo, B. R. Fisher, H.-J. Eisler, and M. G. Bawendi, "Surface-enhanced emission from single semiconductor nanocrystals," Phys. Rev. Lett. **89**, 117401 (2002).

1. Introduction

Since fabrication methods for nanometer sized metal structures with all kinds of geometries are now available, such nanostructures as well as their distinct properties are under intense investigation [1–3]. Besides nanostructures based on periodic geometries [4] also single nanostructures, such as nanoparticles with tailored geometries, offer promising properties for many applications [5, 6]. One concept that is currently intensively investigated is the use of so-called nanoantennas, which are optimized to couple between freely propagating light and tiny localized structures, circuits or molecules of interest [7–11]. Their architectures are inspired by RF analogues and go beyond simple Mie scattering geometries [12]. Since the characteristics of those nanoscale antennas differ strongly from their large microwave counterparts, their properties have to be carefully investigated for applications in the optical regime [13].

The optical properties of such nanostructures, dominated by plasmon resonances, depend strongly on the precise geometry as well as the exact dielectric function of both the structure itself and the surrounding. Small changes in any of these factors can have an essential influence on the performance. On the other hand, fabrication of such small structures is at the limit of what is possible today. One of the major challenges is that during the electron beam fabrication procedure, the proximity effect makes it very difficult to produce sharp edges [14, 15]. Hence, the real fabricated structures differ considerably from ideal structures, intended to be fabricated. Kildishev et al. showed that the surface roughness of nanoantennas has a significant influence on the resonance wavelength and the spectral width of the resonance [16]. However, they did not investigate the influence of deviations in geometric parameters as total length, width, curvatures etc. In another interesting work by Kern et al., the authors showed that realistic nanostructures deviating in all three dimensions from a perfectly rectangular block perform different than the ideal structures [17]. However, the authors did not relate the simulated structure quantitatively

with real measured structures. In a further work by Truegler et al. the influence of the surface roughness of single nanorods was investigated and only small influences were found [18]. In this paper, we use numerical simulation methods to investigate the influence of fabrication uncertainties on the behavior of optical two arm antennas with a nanometer sized gap.

The paper is organized as follows. In Section 2 we present the simulated structures and explain the different configurations for the simulations in Section 2.1. The two applied simulation programs Lumerical [19] and COMSOL Multiphysics [20] are presented in Section 2.2. In Section 3 we discuss our simulation results. In Section 3.1 we demonstrate that the calculated results are adequate by showing a very good agreement between the results from Lumerical and COMSOL. This is followed by an investigation of the near and far field parameters of one particular antenna structure in Section 3.2. Finally we investigate the influence of the fabrication tolerances on the far field parameters for a set of nanoantennas with increasing arm length (Section 3.3). We finish the paper with conclusions in Section 4.

2. Simulations

The resonance wavelength of nanoantennas can be tuned by changing the arm length of the antenna. Since the antenna arm length is the most relevant parameter, the presented investigations are carried out for a set of nine antennas with increasing nominal arm length L from 30 nm to 70 nm in steps of 5 nm. Figure 1 shows scanning electron microscopy images (SEM) taken from these nine antennas, where the actual antenna contours are highlighted in red [23]. As can be seen, significant deviations from the intended geometry - two perfectly rectangular blocks - occur. In the following, we investigate this arm length sweep via simulations at three different level of abstraction, from ideal to realistic antenna structures. In our investigation we do not focus on the average influence of shape deviations as done in other publications as for example [16]. The nine chosen antennas on which the present investigation is based are rather representative samples of real shape deviations of different kinds and intensities. This way, the resonance tuning via arm length changing and the influence of the precise antenna geometry on this resonance tuning can be understood.

(a) L=30 nm	(b) L=35 nm	(c) L=40 nm	(d) L=45 nm
(e) L=50 nm	(f) L=55 nm	(g) L=60 nm	
(h) L=65 nm	(i) L=70 nm		
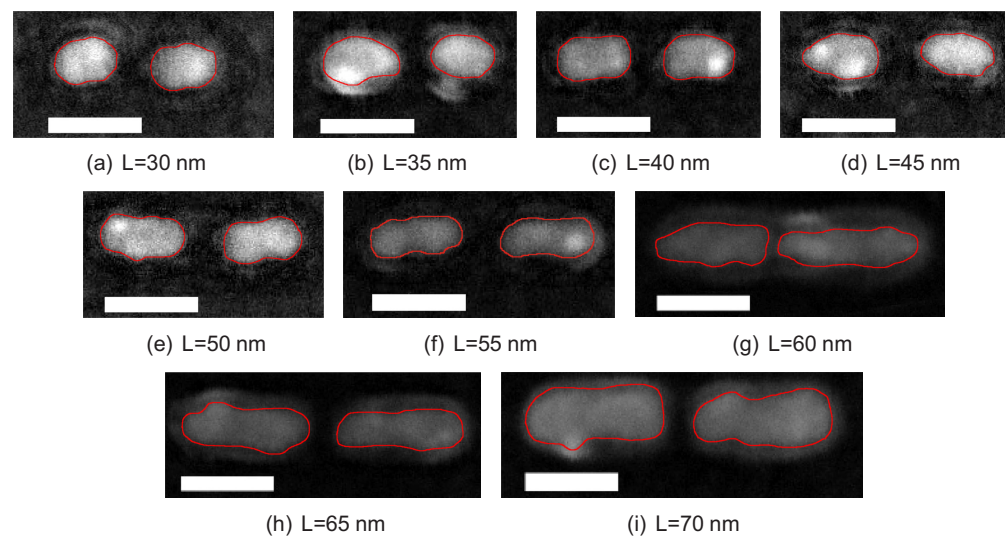
Fig. 1. SEM images of antennas with different nominal arm length L after increasing the contrast [23]. The red curves indicate the extracted contours. Scale bars: 50 nm.
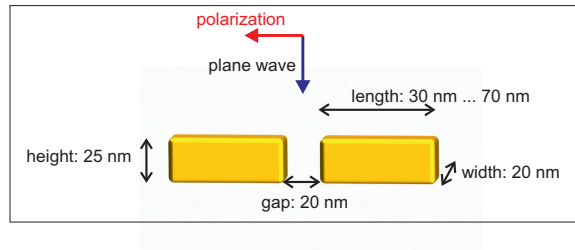
Fig. 2. Simplified sketch of the antenna geometry with a plane wave incident on it (side view).

Figure 2 shows the configuration and dimensions of the intended antenna geometry. One antenna consists of two gold antenna arms (nominal dimensions: height 25 nm; width 20 nm; length 30 nm - 70 nm) separated by a small gap (nominal gap width 20 nm). A plane wave polarized along the long antenna axis is incident on the antenna.

The purpose of this paper is to investigate the influence of the antenna shape on its resonance behavior. Therefore, it is adequate to simulate antennas surrounded by air. Yet, it has to be borne in mind that in reality the nanobars are placed on a substrate (for example glass), which causes a significant red shift of all resonances in comparison to the here simulated cases of antennas in air [data not shown]. As investigated characteristic properties we choose the electric field distribution in the near field of the antenna as well as the two far field parameters scattering cross section and absorption cross section.

2.1. The three different sets of simulations compared in this work
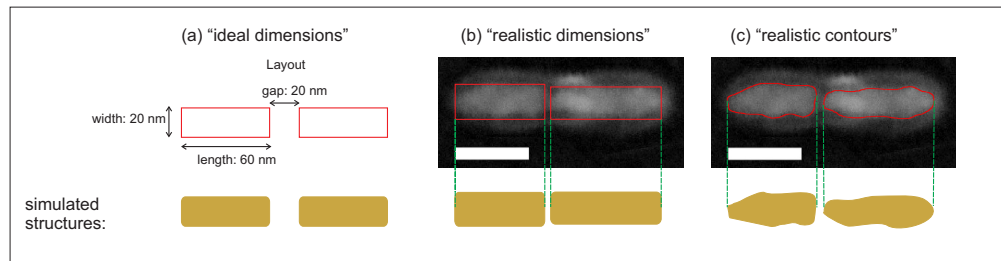
Fig. 3. Simplified sketch of how the three types of simulated structures are obtained (top view). The SEM image is taken from an antenna with nominal arm length of 60 nm (scale bar: 50 nm). All edges are rounded by 3 nm. (a) Dimensions are taken from the layout intended to fabricate. (b) Dimensions are taken from SEM measurements. (c) The contour is extracted from SEM measurements.

Simulations are carried out for three different sets of antenna models. Each set contains nine antennas with the nominal dimensions as depicted in Fig. 2. The difference between the nine antennas is an increasing nominal arm length, ranging from 30 nm in steps of 5 nm to 70 nm. Figure 3 shows how the three different sets of antenna models are obtained. The difference between the three sets is that the first set (Fig. 3(a)) contains ideal geometries, the third set (Fig. 3(c)) contains realistically shaped geometries and the second set (Fig. 3(b)) is an intermediate set included to differentiate between the different origins responsible for the observed deviations. For the first set, called antennas with "ideal dimensions", all dimensions are taken

from the intended layout and correspond to those of Fig. 2. The only modification is that all edges are rounded with a radius of 3 nm. In Fig. 3(b) the set of antenna structures named "realistic dimensions" is obtained by taking the dimensions arm lengths, arm widths, and gap width from an SEM image, but maintaining a cuboid shape. We included this second set of simulations because it is well-known that the optical response of a nanoantenna depends strongly on general geometry parameters as arm length and especially the gap width [21]. Our intension is to differentiate those well-known influences from influences due to the precise contour of the nanoantenna. For the last antenna set (Fig. 3(c)) "realistic contours" the 2D antenna shape is extracted from the SEM image. To obtain a 3D model, the antenna structure is extruded to a constant height of 25 nm.

While modeling the two block shaped types of geometries is straight forward, modeling of the antenna geometries with realistic contours needs some preparation. Figure 4 (left) shows a typical scanning electron microscopy (SEM) image of a nanoantenna fabricated by electron beam lithography. As can be seen, the antenna is surrounded by a "halo". This halo is not part of the real structure. Such halos originate most likely from a contamination with carbon-hydrogen compounds, which can be seen especially well on edges due to the well-known SEM edge-effect [22].
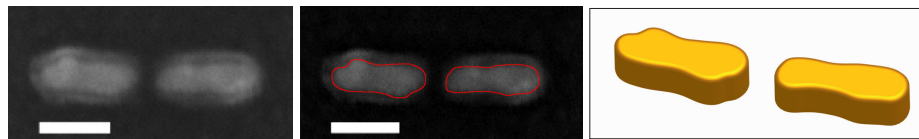
Fig. 4. Left: SEM image of a dipole antenna with a nominal arm length of 65 nm (scale bar: 50 nm). Middle: SEM image with increased contrast. The red line represents the extracted contour. Right: 3D model.

As a first step, we increase the contrast of those images and the structure becomes more visible (Fig. 4, middle). From these images we extract the outlines of the structures manually.

The extracted contour is imported into a CAD program, where it is extruded to a 3D object. The height is estimated to be 25 nm by taking the average from several atomic force microscopy (AFM) images [23]. All edges are rounded with a radius of 3 nm. The resulting 3D CAD model is then imported into COMSOL. Figure 4 (right) shows the final 3D model for an antenna with a nominal arm length of 65 nm.

2.2. *The simulation programs COMSOL Multiphysics and Lumerical*

Simulations are carried out using the Finite Element Method (FEM) [24] based software COMSOL Multiphysics® [20]. With its flexible tetrahedron-shaped mesh, it can favorably reproduce the exact geometry with reasonable calculation effort.

To verify that the simulation results are not affected by numerical instabilities or similar problems, we compare the results obtained with COMSOL Multiphysics to similar simulations done with the simulation software Lumerical [19] which is based on the FDTD method [25]. Since the FDTD method solves Maxwell's equations in the time domain, the whole spectral range of interest can be covered by only one calculation. In contrary to the FEM method, only the use of a cuboid shaped mesh is possible. This makes it less favorable for the simulation of objects with complicated geometries.

In all simulations, the complex dielectric function for gold as measured by Johnson and Christy [26] are used. All antenna models are surrounded by a sufficient number of perfectly matched layers (PMLs).

For the COMSOL Multiphysics simulations we employ the "RF-module". Here, a maximum mesh element size of 6 nm is used for the antenna. In the antenna gap and close to the antenna surface the mesh has a maximum element size of 10 nm. In the remaining area surrounding the structure, the maximum mesh element size is 80 nm. The simulation area has a spherical shape with a radius of 400 nm.

In the simulations carried out with Lumerical, the mesh element size on the antenna is 0.625 nm while it has a maximum element size of 8 nm in the surrounding environment. The simulation domain is cubic here, due to the cubic mesh elements. It has a length of 800 nm in all three dimensions. The simulated time was 150 fs which provided sufficient time after the decay of the incident pulse for stable results.

3. Results and discussion

3.1. Comparison between simulations in Lumerical and COMSOL for antennas with ideal geometries

As a first step, we investigate the adequateness and stability of our simulation results. This is a very crucial point for all further results since the simulation results are easily affected if especially the parameters for the mesh and the PML are not chosen correctly. On the other hand, the calculation time rapidly becomes intolerably long if e.g. a too high mesh resolution is chosen. The following simulation results were obtained with the parameters stated in Section 2.2 and for antennas with ideal dimensions (Fig. 3(a)). In Fig. 5 a comparison of the absorption and scattering cross sections in dependence of the wavelength calculated by the two simulation programs COMSOL and Lumerical is presented. The configuration and all dimensions are as depicted in Fig. 2. Extensive tests regarding the mesh and other simulation parameters have been carried out. It can be seen that the results agree very well. This confirms that the simulations are sufficiently stable. All further results presented in this work have been obtained with FEM simulations in COMSOL.
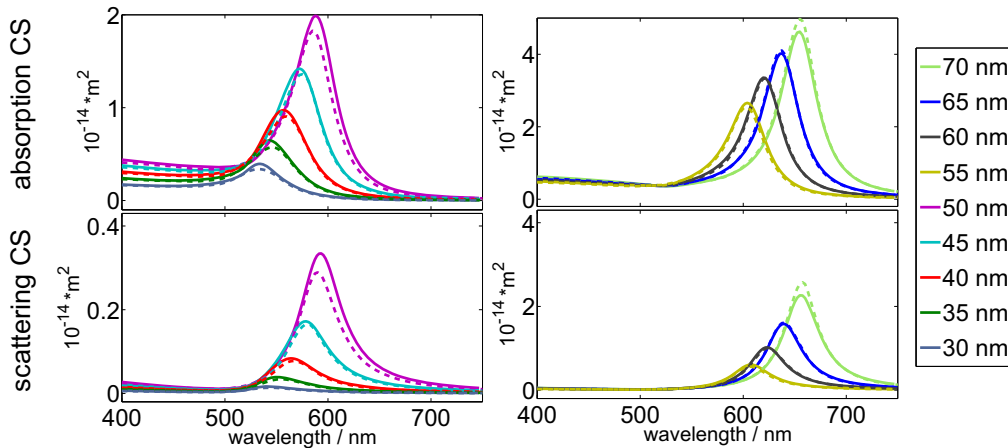
Fig. 5. Absorption and scattering cross sections: comparison of antennas with ideal geometries simulated in Lumerical (solid lines) and COMSOL (dashed lines). Arm length 30 nm - 70 nm (other parameters see Fig. 2).

3.2. Comparison of near and far field properties of one antenna

In this section, the near and far field parameters of the antenna with an arm length of 55 nm are investigated. The field distribution and especially the field enhancement in the near field of the nanoantennas not only serve as a starting point to calculate the antenna's far field response, but are a very important property determining the coupling efficiency to molecules or emitters [8]. The near field distributions of the electric field enhancement for an antenna with ideal dimensions and an antenna with realistic contours are shown in Fig. 6 and Fig. 7.
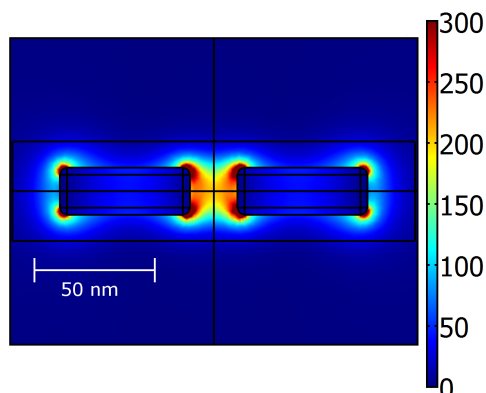
Fig. 6. Near field distribution of the electric field intensity enhancement. The arm length is 55 nm and the wavelength of the incident plane wave is the resonance wavelength of 606.8 nm. The cross section is plotted in the middle of the antenna height. Color bar: $\frac{|E_{tot}|^2}{|E_{in}|^2}$. With E_{in} being the electric field amplitude of the incident plane wave. For this simulation, a finer mesh of maximum element size of 3 nm for the antenna and 5 nm for the close environment is used.
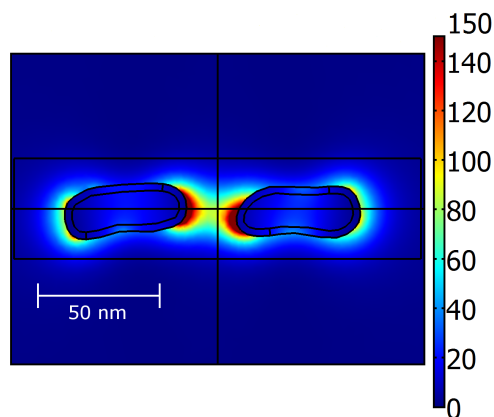
Fig. 7. Near field distribution of the electric field intensity enhancement for an antenna with realistic contours. The nominal arm length is 55 nm and the wavelength of the incident plane wave is the resonance wavelength of 585.5 nm. The cross section is plotted at half of the antenna height. Color bar: $\frac{|E_{tot}|^2}{|E_{in}|^2}$. With E_{in} being the electric field amplitude of the incident plane wave. For this simulation, a finer mesh of maximum element size of 3 nm for the antenna and 5 nm for the close environment is used.

As can be seen, significant deviations between the perfectly rectangular structure in the case of ideal dimensions and the realistic contours structure occur. In this particular case the field enhancement in the antenna gap is significantly smaller in the realistic contours simulation and the field distribution is also altered. We attribute the lower field enhancement of the realistic contour simulation mainly to the lower curvature of the antenna outline at the gap as opposed to the high curvature at the 3 nm rounded edges in the ideal dimensions simulation. Hence, for application where an efficient coupling of nanoantennas to other nanostructures is desired, the precise manufactured geometry is of high importance.

To see how the differences observed in the near field manifest themselves in the far field, we calculate scattering and absorption cross section for the whole spectral range of interest. The results are shown in Fig. 8. Also included are the results of the third type of simulation named "realistic dimensions" where the dimensions are taken from the SEM images but the geometries are still two bars. Again, significant differences between the simulations with ideal dimensions and with realistic contours can be seen. The realistic dimensions simulation helps to better understand the origin of these deviations. This way, the influences of deviation in general geometry parameters - as antenna arm length, antenna width and gap width - are separated from the influences of the precise antenna contour. The results in Fig. 8 show that indeed both influences contribute to the observed deviation.
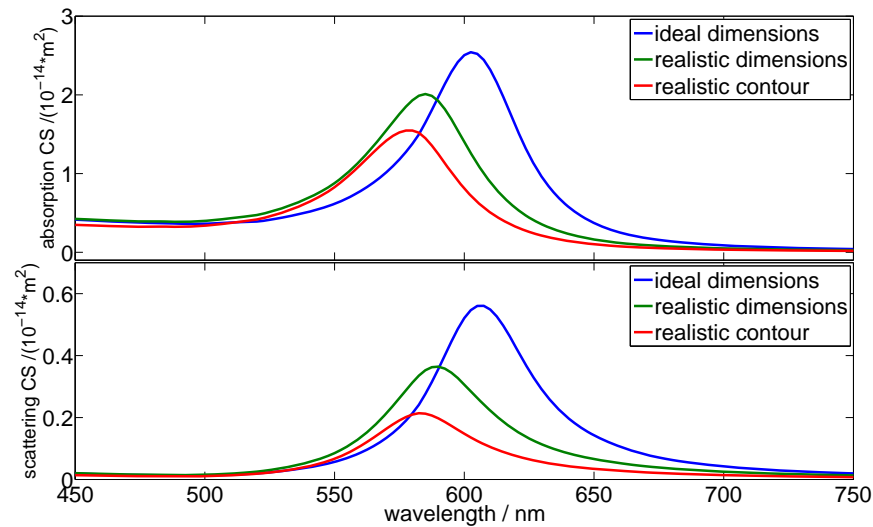
Fig. 8. Absorption and scattering cross sections: comparison between antennas with ideal geometries, realistic dimensions and realistic contours. Arm length 55 nm.

3.3. Comparison of far field properties of antennas with ideal geometries, antennas with realistic dimensions and antennas with realistic contours

The investigations as explained in the previous section are now carried out for all nine antennas with increasing antenna arm length.

For an easier interpretation of the results, we extract the maxima of the respective cross sections as shown in Fig. 8 and plot them versus arm length. This can be seen in Fig. 9. Besides, we also plot the resonance wavelength versus antenna arm length (Fidg. 10). The connecting lines are just a guide to the eye. These two plots are very helpful to understand the influence
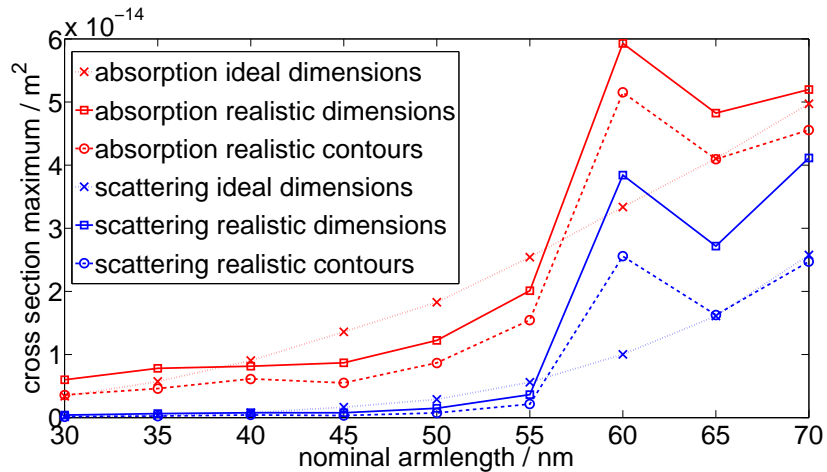
Fig. 9. Maximum of absorption and scattering cross section versus antenna arm length for realistic and ideal geometries.
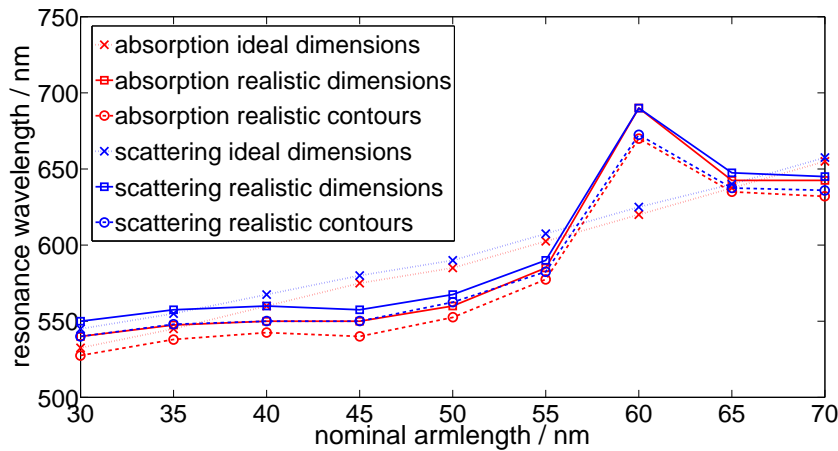
Fig. 10. Resonance wavelength from absorption and scattering cross sections versus antenna arm length for realistic and ideal geometries.

of an ideal antenna arm length sweep and to see how the deviations occurring in manufactured antennas alter this behavior.

Concentrating first on the result for the ideal dimensions (dotted lines, crosses), the expected influence of an increasing antenna arm length on the resonance wavelength and the cross section maxima can be observed [13, 23]. Both cross section maxima increase with increasing arm length. The increase depends on the precise material parameters as well as the shape and aspect ratio of the antenna. The resonance wavelength is linearly red shifted with increasing arm length. These general trends can be observed for the other two sets of simulations, too. Using this illustration, it can also be seen that significant deviations between ideal dimensions and realistic contour simulations (dashed lines, circles) occur for most cases, and that no general trend for this deviation can be observed. Whether the resonance is shifted to higher or lower wave-

length and whether absorption and scattering cross section are increased or decreased depends on the precise geometry of the individual structure.

These differences between ideal dimensions and realistic contours can be investigated by focusing on the results from the antennas with realistic dimensions (continuous line, squares). Two observations can be made. First, the general trend of the curve for antennas with realistic contours is adequately reproduced by the curve for antennas with realistic dimensions. Second, the real contour simulations are generally below the realistic dimension simulations in both resonance wavelength and cross section maximum for both absorption and scattering. There are two major reasons for this general trend. The irregular outlines of the antennas with realistic contours and especially the shape near the antenna gap influence the coupling of the antenna arms and thus the magnitude and wavelength position of the resonance. In addition, for the width and length of the antennas with realistic dimensions, the maximum from the SEM image is taken. Hence, the antennas with realistic dimensions always have a larger volume than the real contour antennas. The differences in the results between realistic dimensions and ideal dimensions let us conclude that fabrication uncertainties can indeed alter general geometry parameters so much that even the optical far field response of the nanoantenna is affected. Of special importance is here the antenna gap, since the coupling between the two antenna arms is highly sensitive to the precise gap width.

A further observation is that, particularly for the two longest antennas, shifts in opposite directions occur: The resonance is shifted to longer wavelengths and higher cross section maxima due to deviation in general geometry parameters, but is shifted to shorter wavelengths and smaller cross section maxima if geometries with realistic contours are used. Hence, results for the realistic dimensions deviate more from the realistic contours than the previously discussed ideal dimensions.

Having a closer look at the results from the sample antennas with a nominal arm length of 60 nm, it can be seen that the differences between ideal geometries and antennas with realistic contours are extremely large. From Fig. 3 and Fig. 1(g) it is clear that the geometry of this particular antenna has very strong deformations and irregularities. Especially, the left arm is much shorter and the antenna gap is nearly closed. It is clear that for such strong deviations a simplified approach is no longer adequate. Having a look at the simulation with realistic dimensions for this particular antenna, it can be seen that the strong deviation can already be reproduced by only considering the deviation in width, length, and gap width from the ideal geometry.

These investigations show that the deviations found between nanoantennas with ideal dimensions and such with realistic contours have two origins. The first is the deviation in general geometry parameters, such as arm length, arm width, and gap width. The second origin for deviations is that the shape of the antenna structure is strongly altered in comparison with an ideal cuboid.

At first glance, the significant differences between the simulations with realistic dimensions and those with realistic contours seem to be contradictory to the results presented in [18] since the authors did not see such a significant influence of shape deviations there. We believe that the main reason for this discrepancy is that especially the coupling between the two antenna arms is mainly influenced by the precise shape of the nanoantenna near the antenna gap. Furthermore, it has to be kept in mind that we do not average results from different shape configurations as done in [16] and partly in [18]. Of course, sample deviations can be much more pronounced than averaged deviations.

We also want to point out that a good agreement of far field parameters from antennas with ideal dimensions and realistic contour structures does not necessarily mean that their near field distributions also agree. For applications based on near field interactions with nanoantennas,

it is thus not sufficient to rely on a good agreement between theoretically calculated far field parameters and experimentally determined far field parameters (which are easier to measure than the precise near field distribution). Numerical simulations as presented in this work can help to get a better understanding of the near field behavior and can complement results from near field measurements based for example on surface enhanced Raman scattering (SERS) [27] or surface enhanced fluorescence (SEF) [28].

4. Conclusions

In this work we investigated the influence of geometrical imperfections in nanoantenna structures. We presented a method how antenna structures with geometries extracted from measured data can be used for a more precise simulation and hence a better understanding of such structures.

We investigated these deviations using a set of sample antennas with increasing nominal arm length. From SEM measurements it can be seen that the investigated nanostructures deviate strongly from the intended geometries. By means of simulations we showed that for nanoantennas with a gap this can lead to significantly different results both in the near field distribution as well as in far field parameters as scattering and absorption cross section. Hence, our findings are highly important for all applications based on near field interactions as well as for applications exploiting the far field properties of nanoantennas. General trends and scaling laws can, however, be learned from simplified structures even for significantly distorted nanoantennas. Furthermore, we showed that the origin of the deviations can be separated into two parts. The first part results from the deviation in general geometry parameters (width, length, gap), while the second part is due to the precise contour of the antenna.